

Comparison of Some Excitation Schemes for a Jet MHD Induction Generator

IGOR R. KIRILLOV* AND EDWARD S. PIERSON†
University of Illinois at Chicago Circle, Chicago, Ill.

An initial analysis of an MHD induction generator operating on a flat, inviscid, pure-liquid jet with the magnetic vector potential specified is presented. The behavior for this model is controlled not by the conventional slips $s = u\alpha/\omega - 1$, where u is the fluid velocity, α the wave number, ω the frequency in rad/sec, and ω/α the velocity of the traveling magnetic field; but by the effective slip $s_e = (u/\omega)[\alpha + x(d\alpha/dx)] - 1$. Numerical and/or analytical solutions for the fluid velocity and powers are obtained for four forms of $\alpha(x)$. The constant α and constant s cases are impractical because of the spatial dependence of the field-fluid interaction. The constant s_e and linear-variation-of- α cases offer the possibility of improved performance with reasonable power densities and the reduction or elimination of viscous losses and ohmic wall losses. This analysis is also applicable to nonjet variable-velocity generators.

Nomenclature‡

A	= vector potential
B	= magnetic flux density
C	= interaction parameter, $\pi\alpha_0^2\sigma_f A_m^2/2\rho_f\omega$
E	= electric field intensity
I_{ex}	= net generator exciting current
I_f	= net generator fluid current
J	= current density
K	= excitation surface current density
L	= generator length
P_m	= mechanical power removed from fluid
P_{m0}	= mechanical power per pole pitch at entrance, Eq. (22)
P_r	= fluid ohmic power loss
P_s	= gross electrical output power
Q	= volume flow rate, $2cb_ju$
R_M	= magnetic Reynolds number, $\mu_0\sigma_f\omega/\alpha^2$
b	= half-spacing between excitation sheets
b_j	= jet half-thickness
c	= jet width
i	= unit vector
j	= $(-1)^{1/2}$
k_r	= demagnetizing coefficient for exciting current
s	= slip based on field phase velocity, $(u\alpha/\omega - 1)$
s_e	= effective slip, $(u/\omega)[\alpha + x(d\alpha/dx)] - 1$
t	= time
u	= x component of fluid velocity
u_s	= field phase velocity, ω/α
v	= fluid velocity
w	= z component of fluid velocity
x	= axis in direction of fluid flow
y	= axis in direction of current flow
z	= axis in direction of magnetic field
α	= wave number, $2\pi/\lambda$
β	= slope of α for linear-variation of α
η_e	= electrical efficiency, P_s/P_m
θ	= angle of demagnetizing coefficient k_r
λ	= wavelength, $2\pi/\alpha$
μ_0	= permeability of free space
ξ	= $2\beta\tau_0^2/\pi$

ρ_f	= fluid mass density
σ_f	= fluid electrical conductivity
τ	= pole pitch, π/α
Φ	= net generator magnetic flux
ω	= frequency in radians per second
∇	= vector differential operator

Subscripts

c	= core variable
m	= amplitude
0	= initial value, $x = 0$
x, y, z	= components of a vector

I. Introduction

IN liquid-metal MHD power systems, the accelerating systems, two-phase nozzles or similar devices, are by their nature sources of kinetic energy. Typical output velocities of the working fluid, which may be either a two-phase (liquid and vapor) mixture or a pure liquid, are well over 100 mps. In the MHD generator this kinetic energy is partially converted into electrical energy, but the most significant loss mechanisms are due to the fluid viscosity (friction losses and circulating-current ohmic losses due to the velocity profile). The use of an upstream diffuser to produce static pressure to drive a constant-fluid-velocity generator is to be avoided, if possible, because of its low efficiency, particularly with two-phase mixtures. Variable-velocity generators, which convert part of the kinetic energy directly into electrical output energy without pressure as an intermediate step, combine the diffuser and generator into one unit. This simultaneously reduces the velocity or viscous loss along the generator and keeps the static pressure low enough to avoid structural problems and added ohmic wall losses. In either the constant-velocity or variable-velocity generators the length must be short to minimize viscous losses, and this increases the significance of end effects. Another approach is to build a generator operating on a flat, two-dimensional jet and thus to virtually eliminate viscous losses and reduce or eliminate ohmic wall losses.

There have been several analyses of MHD jets,¹⁻³ but these have been of jets into liquids rather than vapors. The conversion of energy and the stability of the jet have not been considered. Although the possibility of jet generators has been discussed, the only published study is an experimental investigation of a conduction jet generator.⁴

The MHD induction generator has been considered for many of the proposed power cycles because it generates a.c.

Received December 15, 1969; revision received Aug. 4, 1970.

* Visiting Lecturer at the University of Illinois at Chicago Circle, under the 1968-1969 U.S.-U.S.S.R. Exchange Agreement; now at D. V. Efremov Research Institute for Electrophysical Equipment, Leningrad, U.S.S.R.

† Associate Professor of Electrical Engineering, Department of Energy Engineering.

‡ Rationalized mks units are used. Boldface type indicates a vector, overbars indicate the complex amplitude, an asterisk (*) the complex conjugate, 2 vertical lines, || the magnitude, and tildes (~) a normalized value.

directly at useable voltages, and d.c. to a.c. conversion is not required. The performance of the basic constant-velocity, infinite-length case is now well understood,⁵ and attention has been focused on understanding the various loss mechanisms such as end loss.⁶ The papers presented at the 1968 Warsaw Symposium have shown that, at least in principle, the electrical losses can be made small,⁷ and that viscous loss in the traveling-field region will be the major loss mechanism. There have also been several experimental studies of generators with both constant fluid velocity^{6,8-11} and variable fluid velocity.¹² The jet generator is a logical outgrowth of previous work on the variable-velocity generator,¹³ and offers the possibility of improved performance. The following analysis, although done for a jet generator, is also applicable to a constant-pressure variable-velocity generator with the same conditions.

II. Model and Assumptions

The model to be analyzed, Fig. 1, is a flat, pure liquid jet traveling in the x direction between two parallel excitation sheets spaced a constant distance $2b$ apart. The thickness of the jet parallel to the magnetic field is $2b_j(x)$. The constant liquid properties are an electrical conductivity σ_f , permeability μ_0 (the same as free space), and mass density ρ_f . The jet is electrically infinite in the y or current direction, perpendicular to both the magnetic field and the fluid velocity, and this implies that the sides of the jet are in contact with perfectly-conducting electrodes spaced a constant distance c apart. There is no external electrical connection to the electrodes, they serve only to close the electrical currents in the fluid.

The region above and below the jet is assumed to be filled with vapor at a sufficient pressure to eliminate boiling. This vapor may be circulated to cool the excitation system and to reduce friction losses. Friction between the liquid and the vapor is neglected, as is friction with the electrodes since the contact area is small compared with the total surface area of the jet, $c \gg b$.

The excitation system which produces the traveling magnetic field and transfers power to or from the jet by means of the field, consists of a polyphase winding which is normally inserted into slots in an iron core. This is represented by a surface current backed up by an ideal iron core of infinite permeability and zero conductivity. (Previous analysis has shown that an iron core is required for acceptable performance,¹⁴ and that an ideal core is a very good approximation to an actual core.⁵) In this analysis the vector potential is chosen and the required surface current density is then calculated for an air-gap length $2b = 2b_j(L)$, the jet height at the exit. (The air gap may be tapered to reduce the excitation power.) The resulting surface current will not be a pure traveling sinusoid. It is assumed that an electrically-conducting channel wall between the fluid and the excitation is not required for the jet generator, but electrical wall loss, if required, may be added by known methods.¹⁵ Electrical and/or thermal insulation may be included by increasing b .

The equations to be solved are Maxwell's equations for the electromagnetic field with the usual MHD approximation of neglecting displacement currents, and the momentum and continuity equations for the incompressible fluid. A slit-channel model is assumed, where the magnetic field is z directed and independent of z , because this has previously been shown to give the best performance,⁵ and because it is analytically much simpler. This corresponds to assuming that $2\pi b/\lambda(x)$ is small compared to unity, where $\lambda(x)$ is the wavelength for the magnetic field. The variable wavelength is produced by properly varying the spacing between the slots in the iron core.

The form of the vector potential, defined in terms of the magnetic flux density \mathbf{B} by

$$\mathbf{B} = \nabla \times \mathbf{A} \quad (1)$$

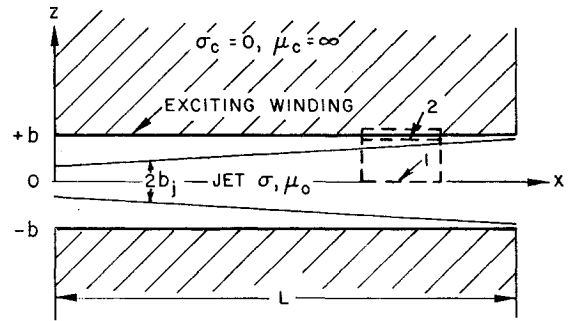


Fig. 1 The model.

is chosen to be

$$\mathbf{A} = \text{Re}\{\mathbf{i}_y \tilde{A}\} = \text{Re}\{\mathbf{i}_y A_m \exp[j(\omega t - \alpha(x)x)]\} \quad (2)$$

where ω is the frequency in radians per second and $\alpha(x) = 2\pi/\lambda(x)$ is the wave number. The vector potential is set because it simplifies the analysis and the boundary conditions. In later solutions the magnetic flux density may be specified. Four different forms will be chosen for $\alpha(x)$.

The machine has already been assumed to be electrically infinite in the y direction and to have fixed parallel side bars, so that there is no y component of the fluid velocity and no y dependence of any parameter. The machine is also assumed to be electrically infinite in the x direction so that end effects due to the jet entering and leaving the traveling magnetic field and due to the open magnetic circuit are not considered. These end effects are not basic to the interaction between the traveling field and the jet, and may be corrected for by the use of compensating poles.⁶ Electrical and viscous losses in the compensating-pole regions are not included.

The form of the fluid velocity can be written as

$$\mathbf{v} = \mathbf{i}_x u(x, z) + \mathbf{i}_y w(x, z) + \mathbf{v}_1(x, z, t) \quad (3)$$

where u and w are the time-average components and \mathbf{v}_1 includes the pulsations due to the time-varying electromagnetic force. The pulsations are assumed to be small and

$$u \partial u / \partial x \gg v \partial u / \partial z \quad (4)$$

so that the time-average momentum equation for the fluid becomes

$$\rho_f u \partial u / \partial x = \frac{1}{2} \text{Re}\{\mathbf{J}_y \tilde{B}_z^*\} \quad (5)$$

where $*$ denotes the complex conjugate, and the viscous and pressure-gradient force densities are negligible for the jet. The fluid current density in terms of the vector potential is

$$\mathbf{J} = \sigma_f (\mathbf{E} + \mathbf{v} \times \mathbf{B}) = \text{Re}\{\mathbf{i}_y \sigma_f (-\partial \tilde{A} / \partial t - u \partial \tilde{A} / \partial x)\} \quad (6)$$

using Ohm's law for the moving fluid and Maxwell's equations for \mathbf{E} . Assumption 4, valid for a slowly-diverging jet, implies that u depends only on x for the consistency of Eqs. (3, 5, and 6). Equation (5) can be rewritten as

$$\rho_f u \frac{du}{dx} = -\frac{\sigma_f \omega A_m^2}{2} \left[\frac{u}{\omega} \left(\alpha + x \frac{d\alpha}{dx} \right) - 1 \right] \left[\alpha + x \frac{d\alpha}{dx} \right] \quad (7)$$

The continuity equation,

$$u b_j = u_0 b_j(0) \quad (8)$$

determines the jet height b_j , where u_0 is the velocity at $x = 0$.

III. Constant Field Velocity

This case is similar to the conventional constant-field-velocity MHD induction machine, where $\alpha(x) = \alpha_0$, a constant, and the electromagnetic field velocity is $u_s = \omega/\alpha_0$. Equation (7) now becomes

$$u du/dx = -(\omega/\pi) C(u - u_s) \quad (9)$$

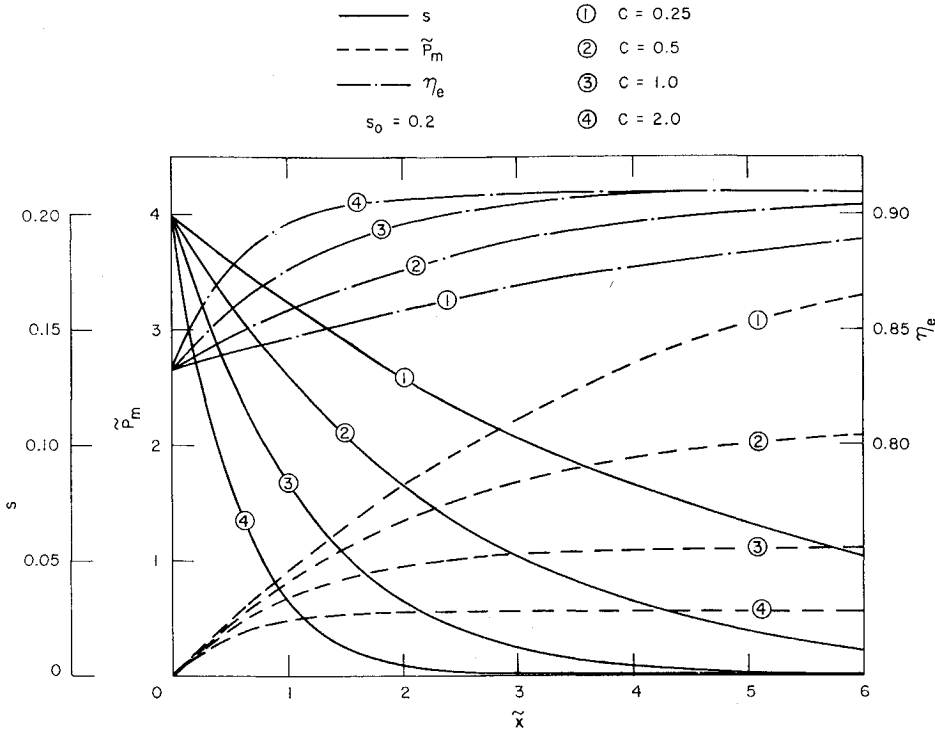


Fig. 2 Slip, normalized mechanical power, and electrical efficiency for constant - field - velocity generator.

where

$$C = \pi \alpha_0^2 \sigma_f A_m^2 / 2 \rho_f \omega = \pi \sigma_f B_m^2 / 2 \rho_f \omega \quad (10)$$

and $B_m = \alpha_0 A_m$ is the (constant) amplitude of the traveling magnetic field. The solution of Eq. (9) in terms of the initial velocity at $x = 0$, u_0 , is

$$u = u_0 - \omega C x / \pi + u_s \ln[(u_0 - u_s)/(u - u_s)] \quad (11)$$

This is written in terms of the slip,

$$s = (u - u_s)/u_s \quad (12)$$

as

$$s = s_0 - C\tilde{x} + \ln(s_0/s) \quad (13)$$

where s_0 is the slip at $x = 0$, $\tilde{x} = x/\tau_0$, and $\tau_0 = \pi/\alpha_0$ is the pole pitch.

The interaction parameter C can be interpreted as

$$C = (F_{em}/F_{in})(1 + s_0)^2/s_0 \quad (10a)$$

where $F_{em} = \sigma_f \omega \tau_0 s_0 B_m^2 / 2\pi$ is the electromagnetic force density at $x = 0$, and $F_{in} = \rho_f u_0 (du/dx)$, which is on the order of $\rho_f u_0^2 / \tau_0$, is the inertial force density of the jet at $x = 0$.

If $u > u_s$, then $(du/dx) < 0$ from Eq. (9), the fluid flow is decelerated, energy is extracted, and the device may be a generator. If $u < u_s$, the flow is accelerated and the device is a pump. The interaction is proportional to s , so that the velocity approaches u_s asymptotically. The maximum ratio of entrance to exit velocities for this case is $(1 + s_0)$, and this occurs only for an infinitely long jet. Since most of the interaction and velocity change occurs in the beginning where s is large, only this part would be utilized in practice.

The mechanical power removed from the fluid by the electromagnetic force, the ohmic loss in the fluid, and the gross electrical output power (the power transferred from the fluid to the excitation system) are

$$P_m = -Q \int_0^L \operatorname{Re} \left\{ \frac{J_y \bar{B}_z^*}{2} \right\} dx = \rho_f \frac{Q}{2} [u(0)^2 - u(L)^2] \quad (14)$$

$$P_r = 2c \int_0^L \left[\int_0^{\tilde{b}_j} \frac{J_y J_y^*}{2\sigma_f} dz \right] dx \quad (15)$$

and

$$P_s = P_m - P_r \quad (16)$$

where $Q = 2cb_f u$ is the volume flow rate. The electrical efficiency, considering only the ohmic loss in the fluid, is

$$\eta_e = P_s / P_m \quad (17)$$

Equations (11) and (13) may be solved exactly only by numerical methods. However, it is possible to find an approximate analytical solution for $s(x)$ by writing Eq. (13) as

$$s = s_0 \exp(-s) \exp(s_0 - C\tilde{x}) \simeq s_0(1 - s) \exp(s_0 - C\tilde{x}) \quad (18)$$

or

$$s = s_0 / [s_0 + \exp(C\tilde{x} - s_0)] \quad (19)$$

Using this gives

$$\tilde{P}_m = \frac{P_m}{P_{m0}} = \frac{1}{s_0} \left[\tilde{x} + \frac{1}{C} \ln \left(\frac{s_0 + \exp(-s_0)}{s_0 + \exp(C\tilde{x} - s_0)} \right) \right] \quad (20)$$

and

$$\tilde{P}_s = \frac{P_s}{P_{m0}} = \frac{1}{2s_0} \left[\tilde{x} + \frac{1}{C} \ln \left(\frac{2s_0 + \exp(-s_0)}{2s_0 + \exp(C\tilde{x} - s_0)} \right) \right] \quad (21)$$

where

$$P_{m0} = b_{j0} c \tau_0^3 \omega^2 \sigma_f s_0 (1 + s_0) B_{m0}^2 / \pi^2 \quad (22)$$

is the mechanical power per pole pitch based on the entrance parameters. The error in the approximate solutions for the slip and powers is less than 5% when $s_0 \leq 0.3$, and less than 10% when $0.3 < s_0 \leq 0.5$. The maximum error in the approximate electrical efficiency is less than 3.2%.

Some results of the exact calculations are presented in Fig. 2 for generator operation. The important feature is that as \tilde{x} increases the slip decreases, and thus the power density or the additions to the total mechanical or gross electrical powers become smaller. With $C = 0.5$ a two-wavelength generator ($\tilde{x} = 4$) has 86% of the infinite-length powers, and for $C = 1.0$ a one-wavelength generator has 85% of the infinite-length powers. Note that the latter is only 35% as long as the former for the same fluid properties and flux density. A further increase in length for these cases is not logical since the gross electrical power will not increase significantly but

Table 1 Ratio of powers for a regular generator to a constant-field-velocity jet generator

n	1.0								2.0				3.0			
	0.25		0.5		1.0		2.0		0.25		0.5		1.0		0.25	
C																
s_0	0.2	0.5	0.2	0.5	0.2	0.5	0.2	0.5	0.2	0.5	0.2	0.5	0.2	0.5	0.2	0.5
P_{mR}/P_{mJ}	1.23	1.18	1.49	1.40	2.13	1.92	3.71	3.28	1.49	1.40	2.13	1.92	3.71	3.28	1.80	1.65
P_{sR}/P_{sJ}	1.18	1.12	1.42	1.27	1.97	1.67	3.40	2.74	1.42	1.27	1.98	1.67	3.40	2.75	1.68	1.46

^a R = regular, J = jet.

the excitation loss is roughly proportional to the length. For a generator to be at least one wavelength long and have a reasonable power density throughout its length, $C \leq 1$. For typical liquid-metal properties of $\sigma_f = 2.24 \times 10^6$ mhos/m and $\rho_f = 726$ kg/m³ (potassium at 500°C), and $B_m = 0.6$ to 1.0 tesla, this implies that the frequency $\omega/2\pi \geq 280$ to 770 hertz.

The powers for the jet constant-field-velocity and the regular constant-field and fluid-velocity generators having the same initial parameters (regular channel height equal to jet initial height) are compared in Table 1, where the subscripts J and R stand for jet and regular, respectively. This jet generator has a much smaller average power density because of its decreasing slip or fluid current, but this is improved later by varying the field velocity. Note that this comparison is not related to a power cycle where the regular generator would be preceded by an upstream diffuser to produce static pressure and thus reduce its fluid velocity relative to the initial fluid velocity of the jet. The jet generator for the same electrical output power may have a larger volume and air gap, resulting in increased excitation loss. The relative total efficiencies of the two generators depend on the reduction in the viscous and ohmic wall losses and the increase in the excitation loss, with the reduction expected to dominate. (The reduction in ohmic wall loss requires correspondingly less excitation current and loss.)

In the three other choices for $\alpha(x)$ the field velocity is varied to prevent the rapid decrease in the power density and improve the performance. This is very significant in that more of the initial kinetic energy of the fluid is utilized, as the constant-field-velocity jet generator is relatively inefficient in this respect.

The required exciting current is determined from

$$\oint_C \mathbf{B} \cdot d\mathbf{l} = \int_S \mu_0 \mathbf{J} \cdot \mathbf{n} da \quad (23)$$

where \mathbf{n} is the normal to the surface. Applying Eq. (23) to contour 1 of Fig. 1 and letting the length of the contour in the x direction approach zero gives

$$K(x,t) = \text{Re}\{\bar{k}_r K_0 \exp[j(\omega t - \alpha_0 x)]\} \quad (24)$$

where K is the y directed excitation surface current density, $K_0 = \alpha_0^2 b A_m / \mu_0$ is the amplitude with no fluid present for this case,

$$\bar{k}_r = k_r \exp(j\theta) = 1 - jR_{M0}s(x)[(s(L) + 1)/(s(x) + 1)] \quad (25)$$

is the demagnetizing coefficient to account for the fluid, and $R_{M0} = \mu_0 \sigma_f \omega / \alpha_0^2$ is the magnetic Reynolds number. Note that $k_r \geq 1$. This expression for \bar{k}_r is valid only for α constant, and is more complex in general.

The numerical solution for \bar{k}_r is shown in Fig. 3 for $R_{M0} = 1$ and 10. Its magnitude is a maximum at the entrance and decreases as the slip and the reaction magnetic field decrease, so that it is less than for a regular generator with the same initial parameters (except at the entrance). For all of the generator cases considered $\theta < 0$, $0.01 < |\theta| < 1.4$ radians, and $|\theta|$ is a maximum at the entrance. The maximum error in \bar{k}_r using the approximate solution, Eq. (19), is less than 7%.

IV. Constant Slip

The field velocity $u_s = \omega/\alpha$ will now vary with the fluid velocity u to hold $s = s_0$. This determines that

$$\alpha = \alpha_0 u_0 / u \quad (26)$$

from Eq. (12), and the momentum equation, Eq. (7), becomes

$$\bar{x}^2 \left(\frac{d\bar{u}}{d\bar{x}} \right)^2 - \left[\bar{x} \frac{1+2s_0}{1+s_0} \bar{u} - \frac{1-s_0}{C\bar{x}} \bar{u}^4 \right] \frac{d\bar{u}}{d\bar{x}} + \frac{s_0}{1+s_0} \bar{u}^2 = 0 \quad (27)$$

in normalized form, where $\bar{u} = u/u_0$. Equation (27) can be solved directly for $d\bar{u}/d\bar{x}$ as a function of \bar{u} , \bar{x} , and constants; but this resulting equation still has to be solved numerically for \bar{u} .

The velocity and powers were calculated numerically from the resulting equation for $d\bar{u}/d\bar{x}$. For every choice of C and s_0 there exists a very short length for which the solution for \bar{u} has a physical meaning. After that length the roots of Eq.

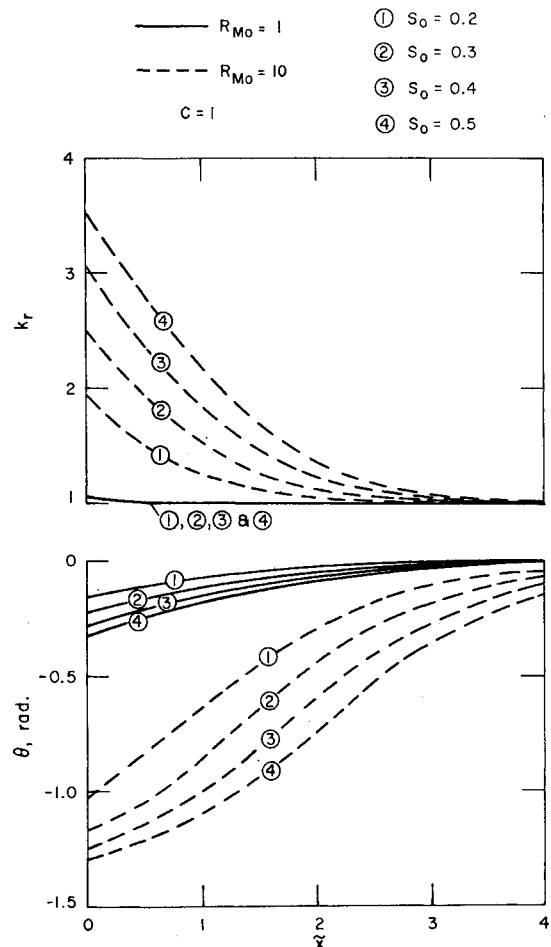


Fig. 3 Demagnetizing coefficient for constant-field-velocity generator with $C = 1.0$.

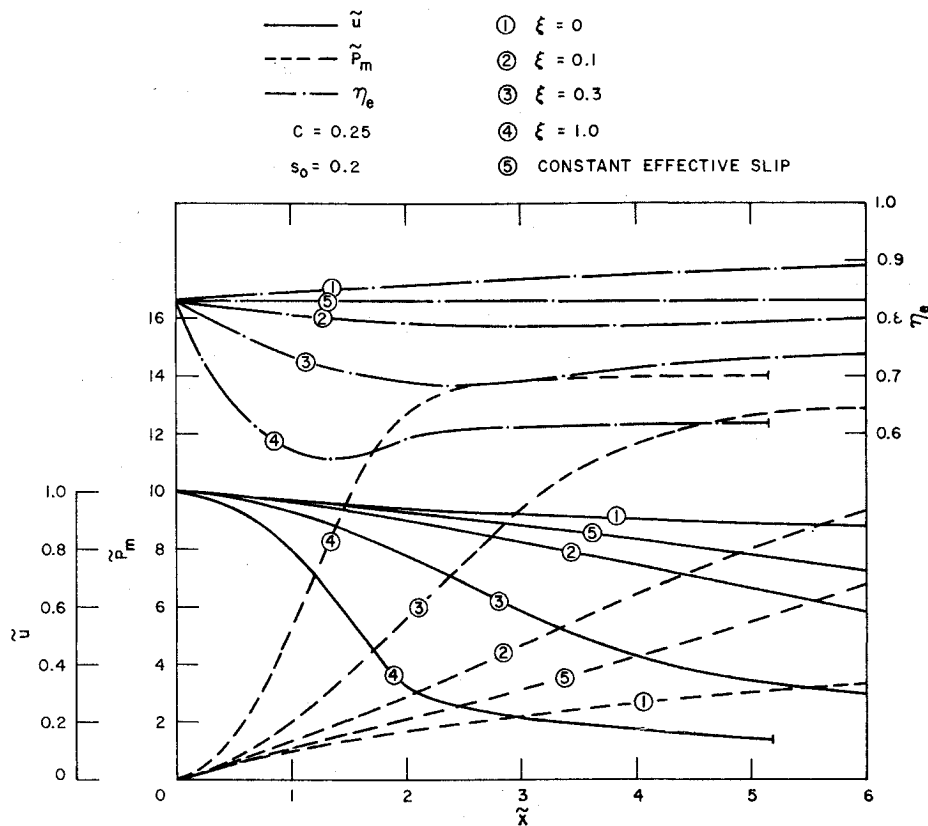


Fig. 4 Normalized velocity, normalized mechanical power, and electrical efficiency for linear-variation-of-wave-number and constant-effective-slip generators for $C = 0.25$ and $s_0 = 0.2$.

(27) for $d\tilde{u}/d\tilde{x}$ become complex. This occurs because the electromagnetic pressure gradient increases rapidly with \tilde{x} , as is shown by rewriting Eq. (7) for this case as

$$\rho_f u \frac{du}{dx} = -\frac{\sigma_f \omega A_m^2}{2} \left[s_0 - \frac{\alpha_0 u_0 x}{\omega u} \frac{du}{dx} \right] \left[\frac{\alpha_0 u_0}{u} \left(1 - \frac{x}{u} \frac{du}{dx} \right) \right] \quad (7a)$$

As x increases, du/dx is negative and u decreases, so that $|du/dx|$ increases until a real solution with this constraint becomes impossible. One reason for the short valid length of the solution is that the vector potential amplitude is constant, and this results in the magnetic flux density growing along the jet.

The maximum length \tilde{x}_m of the real solution for the constant-slip jet generator and $\tilde{u}(\tilde{x}_m)$ is given in Table 2 for

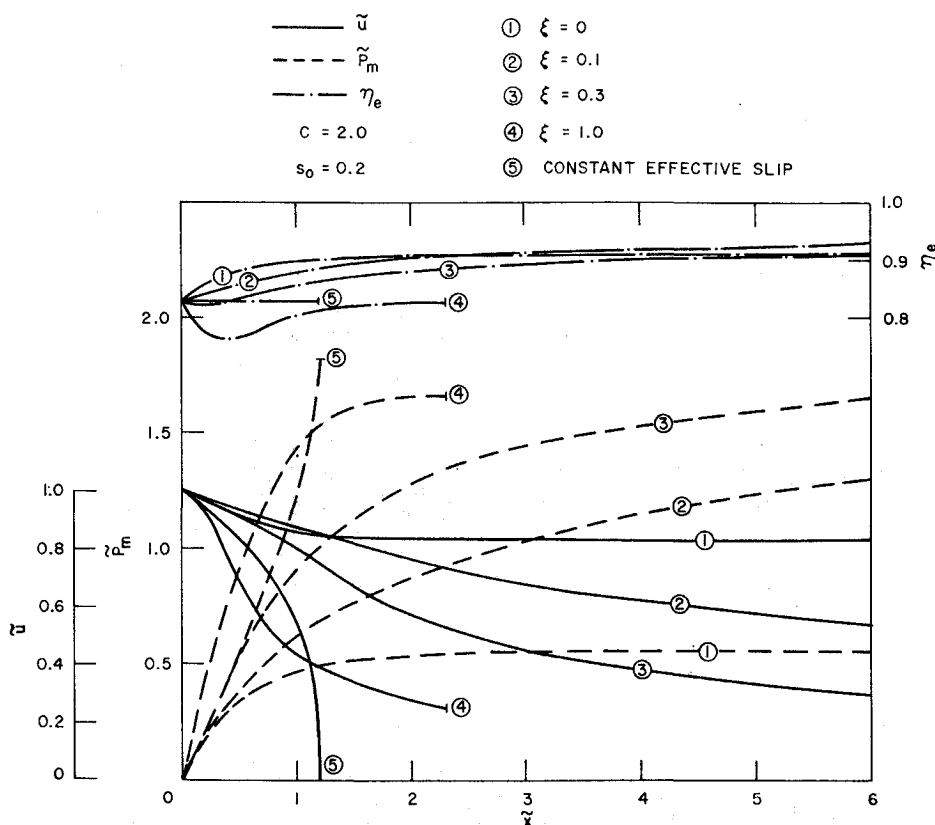


Fig. 5 Normalized velocity, normalized mechanical power, and electrical efficiency for linear-variation-of-wave-number and constant-effective-slip generators for $C = 2.0$ and $s_0 = 0.2$.

Table 2 Maximum length and final velocity for constant-slip solution

C	0.25				0.5				1.0			
s_0	0.1	0.2	0.3	0.4	0.1	0.4	0.1	0.4	0.1	0.4	0.1	0.4
\tilde{x}_m	2.05	1.75	1.60	1.55	1.03	0.78	0.50	0.38	0.93	0.88	0.94	0.89
$\tilde{u}(\tilde{x}_m)$	0.93	0.90	0.89	0.87	0.93	0.88	0.94	0.89	0.93	0.88	0.94	0.89

several sets of C and s_0 . Even a one-wavelength generator is possible only with $C \leq 0.25$, which makes this type of jet generator impractical.

V. Linear Variation of Wave Number

Since for the jet generator with constant field velocity the variation of slip over some length is nearly linear in x , it was decided to try a linear variation of the wave number. Thus, $\alpha = \alpha_0 + \beta x$, where $\beta > 0$ for a generator so that the field velocity decreases. Then Eq. (7) becomes

$$\frac{d\tilde{u}}{d\tilde{x}} = -\frac{C}{1+s_0} \left[(1+\xi\tilde{x})^2 - \frac{1+\xi\tilde{x}}{\tilde{u}(1+s_0)} \right] \quad (28)$$

where

$$\xi = 2\beta\tau_0^2/\pi \quad (29)$$

This equation was solved numerically, and some of the results are given in Table 3 and Figs. 4, 5, and 6.

Before interpreting the results, it is important to note that the characteristics of this generator are determined not by the conventional slip $s = u\alpha/\omega - 1$, but rather by the effective slip

$$s_e = [(u/\omega)(\alpha + x d\alpha/dx)] - 1 \quad (30)$$

The current density in the fluid, Eq. (6), is $J_y = j\sigma_f s_e \omega \tilde{A}$, so that it and the electromagnetic force density, Eq. (5) or (7), reverse sign when s_e reverses sign. The local electrical efficiency, defined as in Eq. (17) except in terms of the power densities, is $(1+s_e)^{-1}$. For the regular generator s appears in these places instead of s_e , so that s_e for the variable-field-velocity generator with constant vector potential amplitude has the same significance that s does for the constant-field-velocity generator, for which case $s_e = s$.

For the variable-field-velocity generator $d\alpha/dx > 0$, so that s is less than s_e , and s becomes negative when s_e is still positive. This makes generator operation possible in the region of negative s . Thus, it may allow the extraction of more energy from the fluid by extending operation to lower fluid velocities. The solution to Eq. (28) was terminated when $d\tilde{u}/d\tilde{x}$ became positive, and this corresponds to negative s_e . The termination is seen for the one set of curves in Figs. 4 and 5.

For any value of C it is possible to choose ξ such that \tilde{P}_m and \tilde{P}_s , the normalized power densities, will be greater for some length of the jet generator than for a regular generator with the same P_{m0} . [For a regular generator $\tilde{P}_m = \tilde{x}$ and $\tilde{P}_s = \tilde{x}/(1+s_0)$.] This occurs because the magnetic flux density is increasing with \tilde{x} , but after some length s_e decreases and the power densities become small. With C constant the electrical efficiency decreases with increasing ξ , as shown in Table 3, and this is due to the increase in s_e .

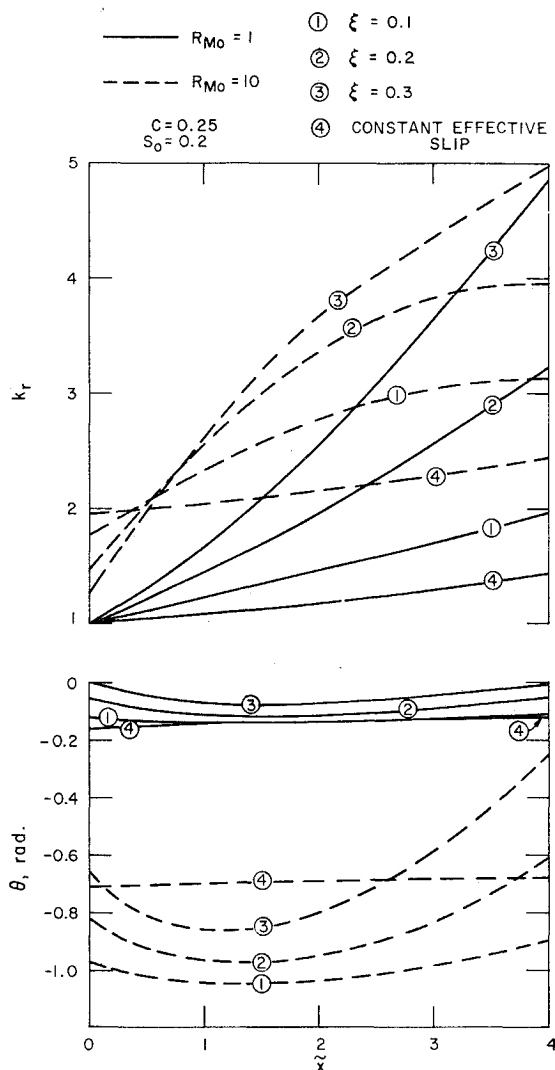


Fig. 6 Demagnetizing coefficient for linear-variation-of-wave-number and constant-effective-slip generators for $C = 0.25$ and $s_0 = 0.2$.

The excitation current density and losses increase with increasing ξ due to the increase in k_r , Fig. 6, and the decrease in the wavelength. (In the definition of k_r , $K_0 = \alpha_0^2 b A_m / \mu_0$ has been retained, but K_0 is now the amplitude of the excitation surface current density with no fluid present only at $x = 0$. Also, Eq. (25) for k_r has to be modified to include the effect of varying α .) Concurrently, \tilde{P}_m increases rapidly with ξ for small \tilde{x} , Figs. 4 and 5. It is apparently possible to choose ξ so that the power density for the jet is equal to or greater than that for the regular generator, and the total efficiency is higher due to the absence of friction and ohmic wall losses. The increase in power density depends on the maximum flux density, but the total efficiency may be greater even though the power density and power output are less.

The electrical efficiency increases with C or B_{m0} increasing, Table 3, due to the greater electromagnetic pressure gradient and consequent reduction in s_e . The excitation power is pro-

Table 3 Results for linear-variation-of-wave-number generators of length $2\pi/\alpha_0$

ξ	0.1				0.2				0.3			
C	0.25	0.5	1.0	2.0	0.25	0.5	1.0	2.0	0.25	0.5	1.0	2.0
\tilde{P}_m	2.83	2.28	1.55	0.88	4.16	3.23	2.07	1.12	5.56	4.10	2.46	1.29
\tilde{P}_s	2.24	1.88	1.35	0.79	3.07	2.53	1.75	1.00	3.85	3.10	2.04	1.13
η_e	0.79	0.83	0.87	0.90	0.74	0.79	0.85	0.89	0.69	0.76	0.83	0.88
$\tilde{u}(\tilde{x} = 2.0)$	0.89	0.83	0.76	0.71	0.85	0.75	0.65	0.61	0.79	0.66	0.57	0.54

portional to B_{m0}^2 because \tilde{P}_m decreases due to the reduction in s_e . This means that there is an optimum value of C which yields the maximum total efficiency. Note that with $C > 1$ the length of the jet with significant power density is small, Fig. 5, so that large C may be impractical.

VI. Constant Effective Slip

This is the only case treated here for which an exact analytical solution can be obtained. Holding s_e constant means that $s_e = s_0 = s_{e0}$ for all x since the two slips are equal at $x = 0$. The use of s_{e0} emphasizes the importance of the effective slip. The normalized momentum equation is

$$\tilde{u}^2 d\tilde{u} = -[Cs_{e0}/(1 + s_{e0})^2] d\tilde{x} \quad (31)$$

and the solution with $\tilde{u} = 1$ at $\tilde{x} = 0$ is

$$\tilde{u} = [1 - 3Cs_{e0}\tilde{x}/(1 + s_{e0})^2]^{1/3} \quad (32)$$

The wave number is

$$\tilde{\alpha} = \frac{(1 + s_{e0})^2}{2Cs_{e0}\tilde{x}} \left[1 - \left(1 - \frac{3Cs_{e0}\tilde{x}}{(1 + s_{e0})^2} \right)^{2/3} \right] \quad (33)$$

from Eqs. (30) and (32), where $\tilde{\alpha} = \alpha/\alpha_0$. The normalized powers are

$$\tilde{P}_m = \frac{(1 + s_{e0})^2}{2Cs_{e0}} \left[1 - \left(1 - \frac{3Cs_{e0}\tilde{x}}{(1 + s_{e0})^2} \right)^{2/3} \right] = \tilde{\alpha}\tilde{x} \quad (34)$$

$$\tilde{P}_r = s_{e0}\tilde{P}_m/(1 + s_{e0}) \quad (35)$$

$$\tilde{P}_s = \tilde{P}_m/(1 + s_{e0}) \quad (36)$$

and

$$\eta_e = 1/(1 + s_{e0}) \quad (37)$$

The power relations again show that s_e substitutes for s in this case. Note that the electrical efficiency goes to unity as s_e approaches zero, but that this is not of practical interest because the generated power, and thus the total efficiency, go to zero.

The maximum length of the constant s_e generator occurs when $u = 0$, or $\tilde{x} = (1 + s_{e0})^2/3Cs_{e0}$. This case allows the greatest extraction of kinetic energy from the flow, although it is impossible to reach $u = 0$ because of power cycle constraints, practical limits on b_j , and because this corresponds to $d\alpha/dx$ infinite.

The power densities for this jet generator are approximately equal to or slightly higher than those for a regular generator with the same initial parameters. (See curve 5 of Figs. 4 and 5 which shows that \tilde{P}_m is greater than proportional to \tilde{x} .) The electrical efficiency is equal to that for a regular generator, but the excitation losses are higher due to the larger air gap, the increased exciting current for $\tilde{x} > 0$, curve 4 of Fig. 6, and the decreased room for the winding. The increased exciting current is required because both the total fluid current and the magnetic field increase with \tilde{x} . The increase in the total fluid current is due solely to the increase in the jet height b_j . Hence the efficiency of this jet generator relative to a regular generator again depends on the reduction in friction and wall ohmic losses and the change in excitation loss.

VII. Comparison of the Four Cases

The constant-field-velocity and constant-slip cases represent the two extremes in terms of the variation of the interaction along the jet. For the constant-field-velocity generator the slip ($s_e = s$ for this case) and the electromagnetic force density decrease as x increases. This can yield a high electrical efficiency due to the low average slip, but a low average power density. The maximum ratio of entrance to exit velocities is $(1 + s_0)$, so that for initial slips of around 0.5, the maximum for an acceptable efficiency, less than 56% of

the initial kinetic energy is available for possible conversion to electrical output energy. This is probably too low for a practical power cycle. This case does not appear to be the best form for the jet generator because of the low average power density and the poor utilization of the initial kinetic energy. The inclusion of the penalties for added generator length, such as extra excitation loss, would strengthen this conclusion.

For the constant-slip, constant-vector-potential jet generator the magnetic flux density, fluid current density, and electromagnetic force density all increase rapidly with x . This results in a short length for which a real solution could be obtained, so that the generator may be too short for practical use. Also the rapidly increasing magnetic flux density means that, since the field at the exit is limited by saturation of the iron core, the entrance field and power density will be small. This case does not appear to be practical, although a future investigation with a constant magnetic flux density is of interest because the behavior will be different with the different constraint.

The jet generator with constant effective slip is very close to a regular constant-field-velocity, constant-fluid-velocity generator. The electrical power density and electrical efficiency will be about the same. The excitation losses may be slightly larger for the jet version—depending on the relative effects of air-gap length, generator length, wall currents, etc.—but the viscous and ohmic wall losses will be decreased.

The jet generator with the linear variation of the wave number is, with the appropriate choice of ξ , similar in performance to the case with s_e constant. Increasing ξ will result in higher power density, lower electrical efficiency, and increased excitation loss.

For the latter two cases it appears possible to achieve an increase in the total efficiency due to the absence of viscous loss and ohmic wall loss. The case with the linear variation of α presents more possibility for optimizing the performance due to the extra variable. For example, for s_e constant, the fluid current density is constant and the magnetic flux density is increasing with x . For the linear α case both the current and flux densities vary along the jet, so that the proper choice of ξ can lead to a more rapid increase in the electromagnetic force density with x .

For both of these cases the maximum practical generator length is limited—by u approaching zero for s_e constant or by s_e approaching zero for the linear variation of wave number. However, the interaction parameter C should be chosen so that the generator is at least one wavelength long.

VIII. Conservation Constraints

The conservation laws for the magnetic flux, the fluid current, and the excitation current must be satisfied either inside of the generator or else by means of external provisions. Otherwise there will be magnetic fluxes and/or currents other than those considered in the analyses, and these would change the calculated performance, most likely by degrading it. For example, for the fluid currents this might occur through the creation of a voltage difference between the electrodes, resulting in added currents inside and/or outside of the generator. (This voltage difference is normally zero if compensation is provided for the effects of the finite magnetic structure length.⁶) This voltage is not desired, and will only reduce the efficiency.

In the jet generator the complex amplitudes of the flux and current densities may be functions of x , so that the conservation requirements for all three cannot, in general, be satisfied simultaneously. For a constant-field-velocity, constant-fluid-velocity generator they are all satisfied if the generator is an integral number of wavelengths long, as is generally true. Consider a jet generator with s_e constant as an analytical solution is available. The net magnetic flux Φ , fluid current I_f , and exciting current I_{ex} as functions of the generator length

L are

$$\Phi = c \int_0^L B_z dx = \operatorname{Re}\{c A_m \exp(j\omega t) [\exp(-j\alpha(L)L) - 1]\} \quad (38)$$

$$I_f = \int_0^L 2b_j J_v dx = \operatorname{Re}\left\{-\frac{\sigma_f s_{\infty} Q A_m}{c(s_{\infty} + 1)} \exp(j\omega t) \times [\exp\{-j\alpha(L)L\} - 1]\right\} \quad (39)$$

$$I_{ex} = \int_0^L 2K dx = \frac{2b}{\mu_0} [B_z(0) - B_z(L)] - I_f = \frac{2\alpha_0 b A_m}{\mu_0} \operatorname{Re}\left\{\exp(j\omega t) \left[j \left(\frac{\exp[-j\alpha(L)L]}{\tilde{u}(L)} - 1\right) + R_{M0} s_{\infty} \tilde{u}(L) [\exp(-j\alpha(L)L) - 1]\right]\right\} \quad (40)$$

where the first expression in each equation is the general equation, the second for I_{ex} comes from Eq. (23), and the last in each is for s_{∞} constant. The first two constraints are satisfied if $\alpha(L)L = 2n\pi$, which is the condition that the generator be n wavelengths long because the quantities will have undergone n sine-like (but not truly sinusoidal) oscillations in space. Under this condition I_{ex} is not zero, although this can be handled by wrapping part of the exciting winding around the outside of the core.

This point is not pursued further, but must be considered for any variable u and/or variable u_s induction generator.

IX. Conclusions

The induction jet generator offers the strong prospect of a higher over-all efficiency due to the reduced viscous and ohmic wall losses as compared to the possible slight increase in the excitation loss (relative to a regular generator). The excitation loss should be less than for a variable-fluid-velocity generator because of the reduced ohmic wall currents. The reduction in the fluid circulating currents due to the velocity profile, and thus the fluid ohmic loss, may also be significant. The behavior of the generator with the magnetic vector potential specified is determined by the effective slip, and this will also occur in similar models of the variable-fluid-velocity non-jet induction generator. In fact, this analysis is also applicable to a constant-pressure variable-fluid-velocity generator with the same conditions.

Of the four cases considered here, only the constant s_{∞} and linear variation of α cases are practical because they have acceptable power densities throughout the generator length.

There is still much theoretical work required on the jet induction generator, besides experimental studies. Other cases must be evaluated, including those with the magnetic

flux density rather than the vector potential constrained. The stability of the jet, and the influence of the magnetic field on this stability, is a whole study in itself. Also requiring consideration are formation of the jet, capture of the jet at the end of the generator, and fitting the jet generator into the complete power cycle.

References

- ¹ Moffatt, H. K. and Toomre, J., "The Annihilation of a Two-Dimensional Jet by a Transverse Magnetic Field," *Journal of Fluid Mechanics*, Vol. 30, Pt. 1, Oct. 1967, pp. 65-82.
- ² Smith, D. C. and Cambel, A. B., "Laminar and Turbulent Magneto-hydrodynamic Free Jet," *The Physics of Fluids*, Vol. 8, No. 11, Nov. 1965, pp. 2107-2109.
- ³ Tsinober, A. B. and Shcherbinin, E. V., "Two-Dimensional Magneto-hydrodynamic Jets," *Magnitnaya Gidrodinamika*, Vol. I, No. 3, 1965, pp. 21-29.
- ⁴ Dmitriyev, K. I. et al., "Investigation of a Liquid-Metal Jet MHD Generator," *Electricity from MHD*, 1968, Vol. III, 1968, pp. 2035-2046.
- ⁵ Pierson, E. S. and Jackson, W. D., "The MHD Induction Machine," TR AFAPL-TR-65-107, May 1966, Air Force Aero Propulsion Lab., Wright-Patterson Air Force Base, Ohio.
- ⁶ Cerini, D. J. and Elliott, D. G., "Performance Characteristics of a Single-Wavelength Liquid-Metal MHD Induction Generator with End-Loss Compensation," *AIAA Journal*, Vol. 6, No. 3, March 1968, pp. 503-510.
- ⁷ "Generator Design and Performance Studies," *Electricity from MHD*, 1968, Vol. III, 1968, pp. 1835-1975; Vol. VI, pp. 3709-3717.
- ⁸ Glukhikh, V. A. and Kirillov, I. R., "Experimental Investigation of Asynchronous MHD Converter with Liquid Metal Rotor at Self-Excitation Regime," *Magnitnaya Gidrodinamika*, Vol. 4, 1966, pp. 107-114.
- ⁹ Rowe, I., Wang, T. C., and Dudzinsky, S. J., "Experimental Results with the Variable Fluid and Field Velocity MHD Generator," *Proceedings of the Eighth Symposium On Engineering Aspects of Magnetohydrodynamics*, AIAA, New York, 1967, pp. 31-32.
- ¹⁰ Ulber, M. and Schulz, T., "Experimental Results with an Inductive Liquid Metal MHD Converter," *Electricity from MHD*, 1968, Vol. III, 1968, pp. 1979-2004.
- ¹¹ Pierson, E. S., "Preliminary Experimental Results from a One-Wavelength MHD Induction Generator," *Proceedings of the Eleventh Symposium on Engineering Aspects of Magnetohydrodynamics*, California Institute of Technology, 1970, pp. 161-164.
- ¹² Rowe, I., "60-Cycle Test Results of the Cascade Generator," *Proceedings of the Ninth Symposium on Engineering Aspects of Magnetohydrodynamics*, AIAA, New York, 1968, pp. 171-174.
- ¹³ Elliott, D. G., "Variable-Velocity MHD Induction Generator with Rotating-Machine Internal Electrical Efficiency," *AIAA Journal*, Vol. 6, No. 9, Sept. 1968, pp. 1695-1702; also *Proceedings of the IEEE*, No. 9, 1968, pp. 1449-1458.
- ¹⁴ Jackson, W. D. and Pierson, E. S., "Operating Characteristics of The M.P.D. Induction Generator," *Magnetoplasma-dynamic Electrical Power Generation*, Rept. Series 4, 1963, The Institution of Electrical Engineering, pp. 38-42.
- ¹⁵ Jackson, W. D. and Pierson, E. S., "Material Limitations in the MHD Induction Generator," *Electricity from MHD*, 1966, Vol. II, 1966, pp. 983-993.